Supplement of The Cryosphere, 11, 2329–2343, 2017
https://doi.org/10.5194/tc-11-2329-2017-supplement

The Cryosphere

Supplement of

Spatiotemporal patterns of High Mountain Asia's snowmelt season identified with an automated snowmelt detection algorithm, 1987–2016

Taylor Smith et al.

Correspondence to: Taylor Smith (tasmith@uni-potsdam.de)

Properties of Passive Microwave Sensors

Table S1 – Characteristics of PM sensors. Temporal coverage, number of orbits, and processing algorithms.

Satellite	Temporal Coverage	Number of Orbits Used (Descending/Ascending)	Processing Level/Algorithm
SSMI (Wentz, 2013)	Aug 1987 - Apr 2009 (22 years)	176,460/176,460	FCDR V07
SSMI/S (Sun and Weng, 2008)	Jan 2008 - Apr 2015 (7 years)	41,896/41,896	FCDR V07
AMSR-E (Ashcroft and Wentz, 2013)	May 2002 - Oct 2011 (9 years)	49,083/49,079	L1B
AMSR2 (Imaoka et al., 2010)	Jul 2012 - Oct 2016 (4 years)	28,510/28,506	L1R
GPM (GPM Science Team, 2014)	Feb 2014 - Oct 2016 (2.5 years)	7,359/7,359	L1B

Flowchart of Melt Tracking Algorithm

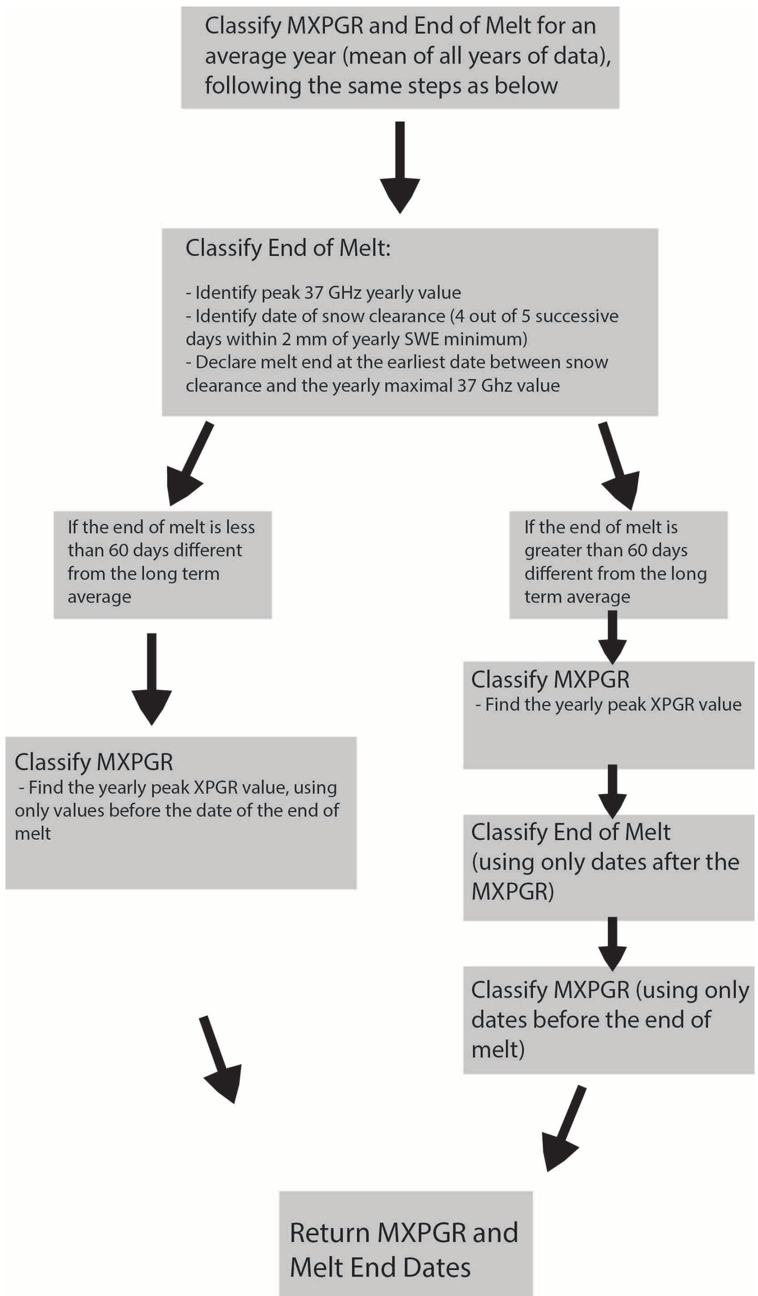

Figure S1 – Flowchart illustrating the steps for the melt tracking algorithm. A full description of the algorithm implementation is maintained on Github: https://github.com/UP-RS-ESP/SnowmeltTracking.

Algorithm Theoretical Considerations

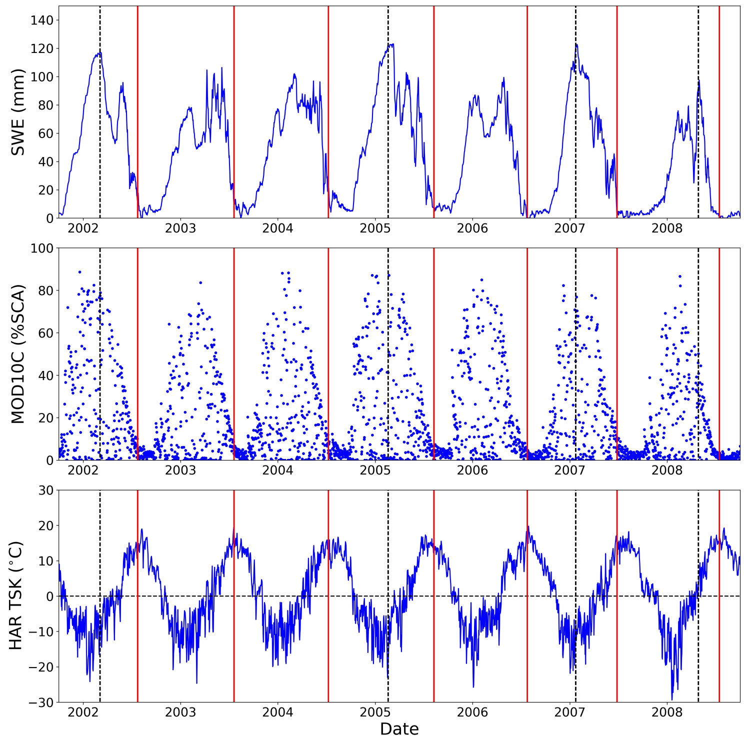

Figure S2 – (A) SWE, (B) MOD10C1 fractional snow-covered area, and (C) HAR daily average temperature. Melt dates in red, with MXPGR as dashed lines and snowmelt end as solid lines. Some years do not have a defined MXPGR date due to complex yearly SWE distributions. MXPGR dates generally correlate with the maximum MODIS snow-covered area and the point where the yearly temperature curve minimizes. End dates correlate well with MODIS snow clearance. Data taken from 71.25E, 36.75N.

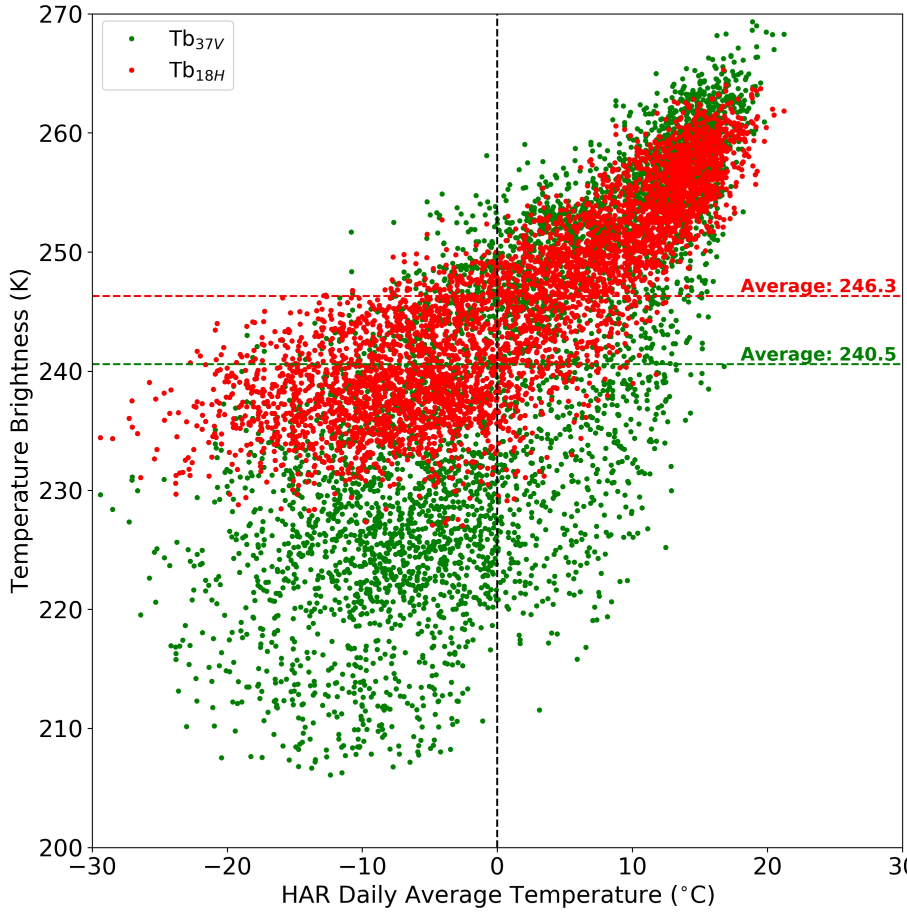

Figure S3 – HAR Average daily temperature vs Temperature Brightness (37V in green, 18H in red, 2000-2014). Both channels show correlations with air temperature, but show a wide spread. This observation indicates that there is no single Temperature Brightness threshold that can be used for snowmelt detection. Data taken from 71.25E, 36.75N.

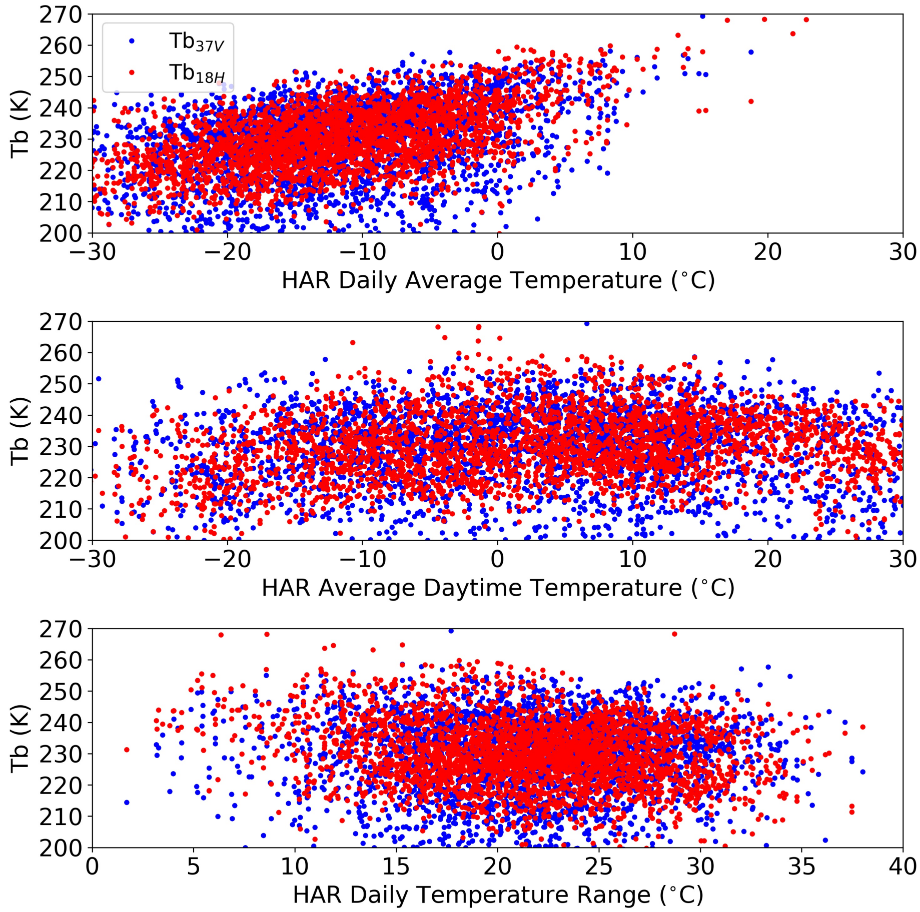

Figure S4 – HAR temperature metrics vs Tb at MXPGR. Both 37V (blue) and 18H (red) channels show significant spread. While there is a slight correlation between average daily temperature and Tb, average daytime temperature is very poorly related to Tb. This implies that the night-time passive microwave data used to identify MXPGR still captures the impacts of above-zero daytime temperatures. Data taken from 71.25E, 36.75N.

Standard Deviation in Snowmelt Period

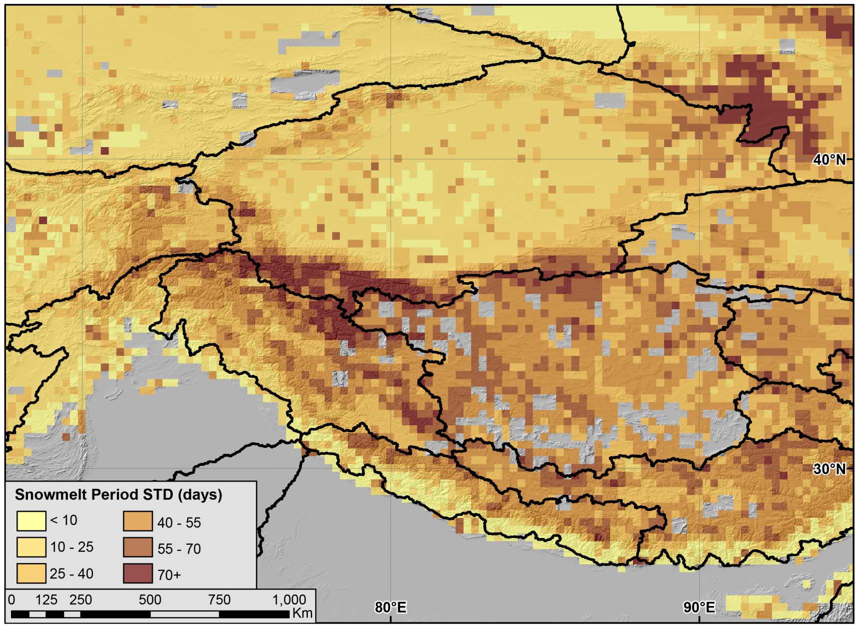

Figure S5 – Standard deviation in snowmelt period, showing higher snowmelt period variance at high elevations and in the orogen interior.

Linear Matching Regression Parameters

Table S2 – Linear matching parameters and statistics - SSMI to AMSR.

SSMI-AMSR			
37V	intercept	Mean	-19.63360131
		STD	35.83495628
		Range	1081.194363
37V	slope	Mean	1.080532984
		STD	0.144976002
		Range	4.12275082
37V	pval	Mean	5.61E-08
		STD	4.82E-06
		Range	0.000413347
37V	tval	Mean	208.7706349
		STD	75.80889139
		Range	476.9591168
18H	intercept	Mean	-21.99749485
		STD	39.91555202
		Range	1140.206255
18H	slope	Mean	1.095758046
		STD	0.164415637
		Range	4.199488203
18H	pval	Mean	1.30E-05
		STD	0.000790001
		Range	0.052541412
18H	tval	Mean	179.2705257
		STD	76.37323937
		Range	435.2829973

Table S3 – Linear matching parameters and statistics - SSMI to SSMIS.

SSMI-SSMIS			
37V	intercept	Mean	-11.82749674
		STD	26.99365273
		Range	1003.134398
37V	slope	Mean	1.046288015
		STD	0.112876411
		Range	4.118598352
37V	pval	Mean	6.75E-15
		STD	5.79E-13
		Range	4.97E-11
37V	tval	Mean	144.7377425
		STD	69.50580512
		Range	393.2536574
18H	intercept	Mean	-22.01065617
		STD	25.4825934
		Range	1003.973949
18H	slope	Mean	1.117712032
		STD	0.115147016
		Range	3.822440322
18H	pval	Mean	0.000122152
		STD	0.010421198
		Range	0.894333768
18H	tval	Mean	138.697067
		STD	74.55722512
		Range	396.2607783

Table S4 – Linear matching parameters and statistics - SSMIS to AMSR2.

SSMIS-AMSR2			
37V	intercept	Mean	-27.90708304
		STD	41.87667407
		Range	995.3410873
37V	slope	Mean	1.113591021
		STD	0.167733559
		Range	3.989960318
37V	pval	Mean	2.24E-17
		STD	1.92E-15
		Range	1.65E-13
37V	tval	Mean	166.7653894
		STD	62.51960823
		Range	398.7550507
18H	intercept	Mean	-32.35079224
		STD	45.3924612
		Range	1048.955192
18H	slope	Mean	1.134449236
		STD	0.188178861
		Range	3.882513428
18H	pval	Mean	3.07E-05
		STD	0.001843432
		Range	0.128179745
18H	tval	Mean	140.8474188
		STD	63.12218532
		Range	459.9962559

Table S5 – Linear matching parameters and statistics - AMSR2 to GPM.

AMSR2-GPM			
37V	intercept	Mean	-4.109791938
		STD	35.93862943
		Range	936.9121798
37V	slope	Mean	1.020145353
		STD	0.144607908
		Range	3.781385974
37V	pval	Mean	2.72E-19
		STD	2.19E-17
		Range	1.87E-15
37V	tval	Mean	79.40991596
		STD	27.93838517
		Range	193.4060824
18H	intercept	Mean	-3.172099946
		STD	41.4648854
		Range	989.3588298
18H	slope	Mean	0.99499014
		STD	0.166546112
		Range	3.592560572
18H	pval	Mean	3.14E-29
		STD	2.69E-27
		Range	2.31E-25
18H	tval	Mean	73.89142489
		STD	29.09024642
		Range	263.9399874

Hierarchical Clustering Metrics

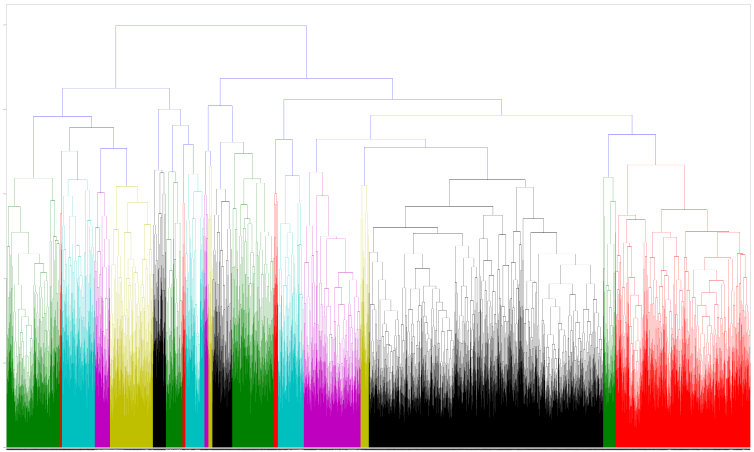

Figure S6 – Hierarchical clustering dendrogram. Clustering performed over Gaussian normalized XPGR values for the entire length of the study period. Methods described in detail in the Manuscript.

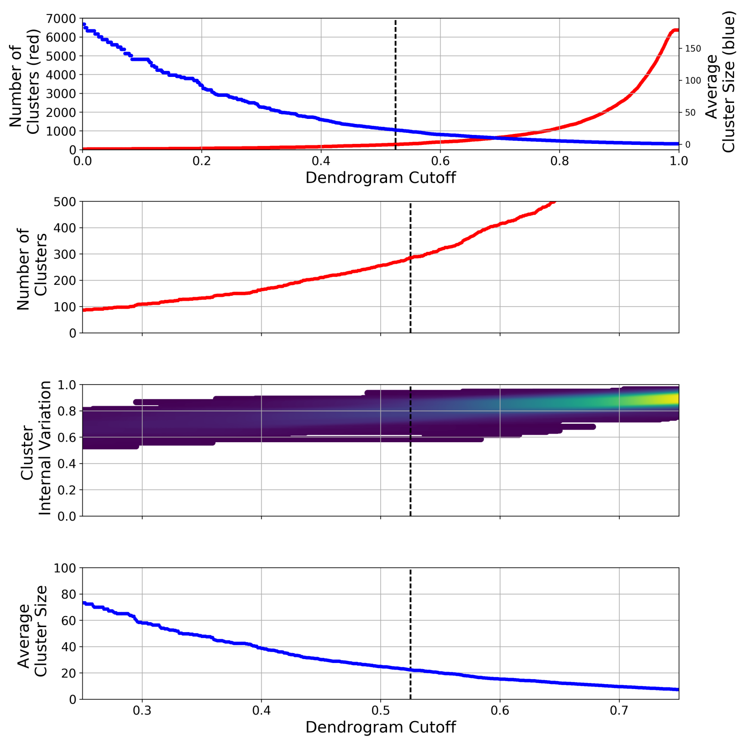

Figure S7 – Metrics used to choose the hierarchical clustering distance threshold. Chosen threshold shown on each chart in black.

Impact of Analysis Timeframe

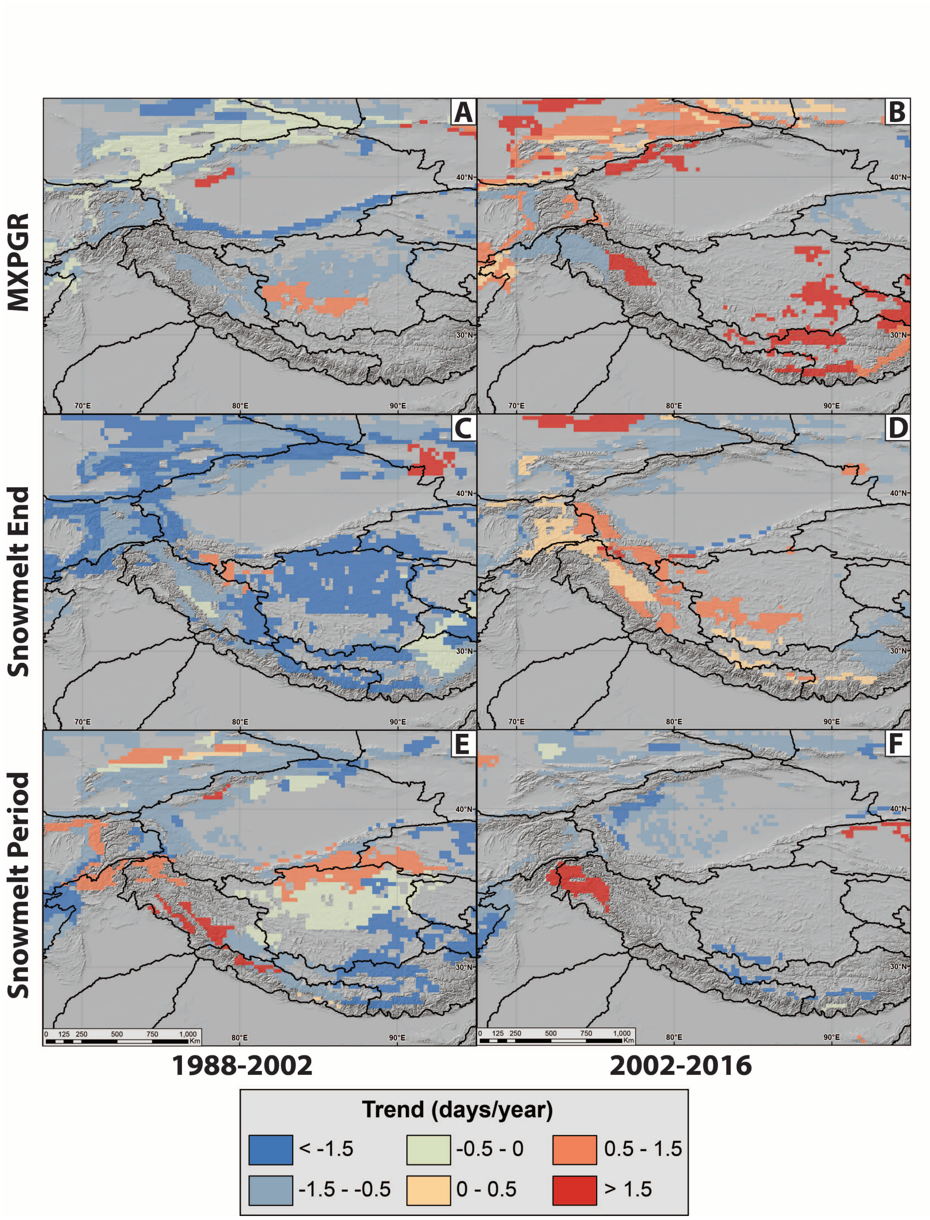

Figure S8 – Impact of analysis timeframe on (A, B) MXPGR, (C,D) snowmelt end, and (E,F) snowmelt period. The MXPGR and snowmelt end dates show a reversal of trend in many regions, from negative to positive.

Bibliography

Ashcroft, P. and Wentz, F.: AMSR-E/aqua L2A global swath spatially-resampled brightness temperatures V003, [2002–2010]., Boulder, Colorado USA: National Snow and Ice Data Center, 2013.

GPM Science Team: GPM GMI Level 1B Brightness Temperatures, version 03, Greenbelt, MD, USA: NASA Goddard Earth Science Data and Information Services Center (GES DISC), 2014.

Imaoka, K., Kachi, M., Kasahara, M., Ito, N., Nakagawa, K., and Oki, T.: Instrument performance and calibration of AMSR-E and AMSR2, International Archives of the Photogrammetry, Remote Sensing and Spatial Information Science, 38, 13–18, 2010.

Sun, N. and Weng, F.: Evaluation of special sensor microwave imager/sounder (SSMIS) environmental data records, Geoscience and Remote Sensing, IEEE Transactions on, 46, 1006–1016, 2008.

Wentz, F. J.: SSM/I version-7 calibration report, Remote Sensing Systems Rep, 11012, 46, 2013.